Isomerization of Antitumour Bicyclic Hexapeptide, RA-VII from *Rubia Cordifolia*. Part 4.[1] Conformation–Antitumour Activity Relationship

Hideji Itokawa,[a,*] Hiroshi Morita,[a] Kazuyuki Kondo,[a] Yukio Hitotsuyanagi,[a] Koichi Takeya[a] and Yoichi Iitaka[b]

[a] *Department of Pharmacognosy, Tokyo College of Pharmacy, Horinouchi 1432-1, Hachioji, Tokyo 192-03, Japan*

[b] *Faculty of Medicine, Teikyo University, Ohtsuka 359, Hachioji, Tokyo 192-03, Japan*

A bicyclic hexapeptide, RA-VII, isolated from *Rubia cordifolia*, has been isomerized under basic conditions to give four derivatives (compounds **1**–**4**). In compounds **1** and **2**, both Tyr-5 and -3 residues were isomerized to give an energetically more favourable alternate D and L amino acid peptide sequence and in compounds **3** and **4**, a Tyr-5 residue was isomerized. Conformational analyses of compounds **1**–**4** in solid and solution states were conducted by X-ray and NMR analysis. The *N*-methyl amide bond between D-Tyr-5 and Tyr-6 is *trans* in compounds **1**–**4**. The geometry of the amide bond on the turn at residues 2 and 3, which is considered to play an important role in the antitumour activity, was found to be *trans* in compounds **1** and **2**, and *cis* in compounds **3** and **4**. Compounds **3** and **4** shows antitumour activities. The conformation of the *cis N*-methyl amide bond between residues 2 and 3 is shown to play an important role in the antitumour activities of RAs.

A series of antitumour bicyclic hexapeptides, RAs (RA-I–RA-XIV,[1–6] RAI-III and RAI-VI)[7] from *Rubia cordifolia* have been characterized structurally by NMR spectroscopic or X-ray diffraction studies and the major active principle, RA-VII (Fig.1), is now being tested for its clinical usefulness. Previously, we worked on the conformations of RAs in solution and solid states, using the latest techniques in NMR spectroscopy and computer simulations,[5,8,9] and showed that the main active principle, RA-VII, existed in two stable conformational states in apolar solvents, *e.g.* in $CDCl_3$. It was also shown that each conformer adopted a stable antiparallel β-sheet conformation with two intramolecular hydrogen bonds between Ala-4 and D-Ala-1. This phenomenon might have resulted from the isomerization about the *N*-methyl amide bond between Ala-2 and Tyr-3 with an isomerization rate slow enough to give separate signals in the NMR spectra. The main conformer A, which was considered to be biologically active, possesses a type II β-turn, involving the residues 2 and 3 with the aromatic side chain of Tyr-3 bent over this turn. The rigidness of the aromatic chain of Tyr-3 was considered to play a very important role in its cytotoxic activity.[5] However, the question as to whether the active principle was the major conformer with a type II β-turn or the minor conformer with a *cis N*-methyl amide bond between the residues 2 and 3 (type VI β-turn) has not yet been answered.

These stable antiparallel conformational forms, however, contain two β-turn structures which cause a strong steric repulsion between the carbonyl oxygen at residue 2 and the side chain at residue 3, and between Hα at residue 5 and Hα at residue 6, these two β-turns being stabilized by the formation of 4-1 type intramolecular hydrogen bonds. Furthermore, a steric repulsion is also present between Ala-4-CH_3 and Tyr-5-NCH_3. RA-VII, having such a constrained conformation, characteristic of the RA series, was found to isomerize easily under basic conditions to compounds conformationally more stabilized, for example, by the formation of 3-1 type intramolecular hydrogen bonds (γ-turn). Two such isomerized compounds, having a type VI β-turn between residues 2 and 3, showed antitumour activities. We believe that studies on the molecular conformations of RAs and the effect of the geometry of three *N*-methylated amide bonds on its conformation will provide some basic information needed for the elucidation of its biochemical

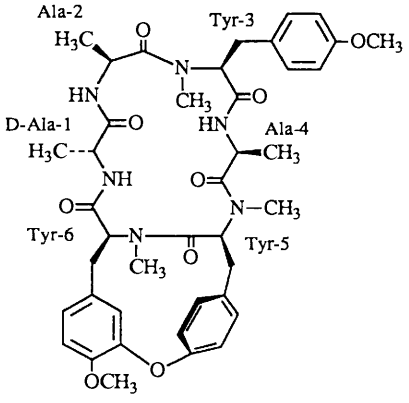

Fig. 1 Molecular structure of an antitumour bicyclic hexapeptide, RA-VII, from *Rubia cordifolia*

functions and that the conformational features of *cis*- and *trans*-isomers may be related to its binding to 80S ribosome.[10] This paper deals with the solid and solution state molecular structures of the four isomerized components (compounds **1**–**4**) produced under basic conditions, and the importance of the *cis N*-methyl amide bond between residues 2 and 3 for the antitumour activities of RAs.

Results and Discussion

Alkaline Isomerization of RA-VII to Compounds **1**–**4**.—RA-VII was treated with 30% $KOCH_3$ in MeOH. The isomerization product was purified by octadecyl silica (ODS) HPLC to give three compounds **1**, **2** and **3** (81, 2 and 8%, respectively). When this reaction was carried out in DMSO solution, compounds **1**, **3** and **4** were formed (55, 7 and 20%, respectively). Compounds **1**–**4** have the same molecular formula, $C_{41}H_{50}N_6O_9$, showing molecular ion peaks at *m/z* 770 in the MS spectra. The amino acid analysis of the four compounds by separation of optical isomers of Dns derivatives using the mixed chelate complex[11] L-His-Cu^{II} showed that they all contained D-Ala:L-Ala in a ratio of 1:2 as in RA-VII. Therefore, the structural difference between these four compounds and the parent RA-VII was considered to be in the configuration of the three *N*-methyl

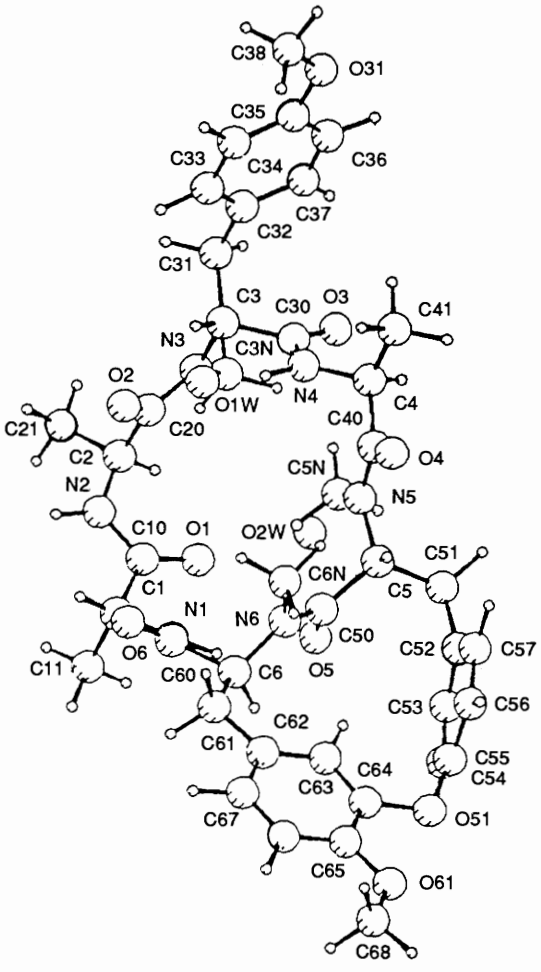

Fig. 2 A perspective view of the crystal structure of compound 1 by PLUTO drawing. Each number refers to the carbon, oxygen and nitrogen atoms of compound 1.

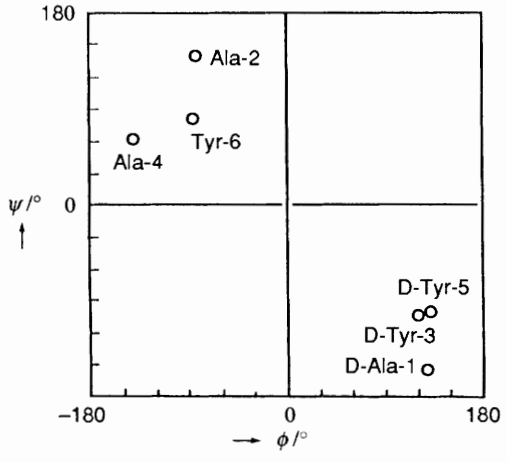

Fig. 3 Ramachandran plot of compound 1, φ and ψ angles of compound 1 calculated by X-ray diffraction

tyrosine units and/or the conformational states. The ^1H and ^{13}C NMR spectra of compounds 1–4 showed quite different features from those of RA-VII. RAs are known to produce characteristically two or three conformational states by isomerization about one or more *N*-methyl amide bonds.[8,9] However, compounds 1–4 apparently exist only in one conformational state in both $CDCl_3$ and [$^2H_6$]DMSO.

X-Ray Analysis of Compound 1.—Firstly, to determine the whole structure and conformation of main compound 1 in the solid state, X-ray diffraction analysis was undertaken. Compound 1 was crystallized from MeOH solution in orthorhombic crystals of space group $P2_12_12_1$. Fig. 2 shows the backbone of compound 1 in a perspective view. In Fig. 3, the φ and ψ angles are summarized in the Ramachandran plot,[12] which shows that all the amino acids have the (φ, ψ)-values in the energetically favourable β-region and that L- and D-amino acids are linked together alternately in the peptide ring. The characteristic feature of RAs having both an 18-membered peptide ring and a 14-membered ring formed by the oxidative coupling of the phenolic oxygen exists also in compound 1. Table 1 shows the backbone dihedrals in compound 1, RA-VI[5] and RA-V-*p*-bromobenzoate.[7]

All of the three structural constraint points of RAs are, as indicated before, in more stable conformational states in compound 1, as evidenced by the three interatomic distances shown in Table 2. One important effect caused by the introduction of one *trans* amide group into the centre of the turn is a significant increase in the distance between Tyr-5-Cα (C5) and Tyr-6-Cα (C6) atoms (3.855 Å) across the *trans* amide bonds in compound 1, compared with that across the *cis* bonds in RA-VI and -VII (2.9 Å).[13] Further, the repulsive force between Ala-2-CO and the Tyr-3 side chain, which is characteristic of RA-VII, represented by the distance between Ala-2-CO (O2) and Tyr-3-Cβ (C31), no longer existed in compound 1 and RA-VI, because Tyr-3 is in the D-form in them. The distance between Ala-4-Cβ (C41) and Tyr-5-NCH_3 (C5N) is much longer than the corresponding distances in RA-VI and VII.

Cyclic peptides are constrained as they contain turns in their backbones and these turns are often stabilized by intramolecular hydrogen bonds. Such structures may provide good models for studies of various possible types of turn containing intramolecular hydrogen bonds and for establishing the molecular dimensions and conformational angles of such turns. As shown in Table 3, the conformation of crystalline compound 1 is stabilized not by a 4-1 type hydrogen bond (β-turn), characteristic of RAs, but by a 3-1 type hydrogen bond (γ-turn) between D-Ala-1-NH and Tyr-5-CO, involving seven atoms. While β-turns are a common occurrence in proteins and peptides, γ-turns are less frequent. The γ-turn as a possible feature of polypeptide and protein conformations was proposed firstly by Nemethy *et al.*[14] and has been observed in several instances in small cyclic peptides containing a proline.[15,16] An interesting feature of γ-turns is the twisting away of the amide bond in the second peptide unit, from a *trans* planar conformation with a ω value of 14–24°,[16] whereas the ω value of the γ-turn in compound 1 is only 3.6°. This unusual ω value is considered to be caused by the highly constrained 14-membered ring system including the isodityrosine unit.

Complete Assignments of ^1H *and* ^{13}C *NMR Signals of Compounds* 1–4.—To obtain information about the structures and conformations, the assignments of ^1H and ^{13}C NMR signals for compounds 1–4, were made by a combination of ^1H–^1H COSY, HMQC[17] and HMBC[18] spectra (Tables 4 and 5).

In the ^1H resonances of compound 1, the chemical shifts of D-Tyr-3-Hα and D-Tyr-3-NCH_3 were similar to those of RA-VI, in which Tyr-3 was of D-form. However, the high field chemical shift of Ala-2-CH_3 was influenced by the anisotropic effect of the D-Tyr-3 aromatic ring. The ^1H signal of Tyr-5-NCH_3 showed a high field shift caused by the anisotropic effect of Tyr-5-CO. In the case of compound 2, the ^1H signals were generally similar to those of RA-VI, but, there are some broad signals around the aromatic rings at 303 K. Such broad signals of compound 2 sharpened at a lower temperature (273 K, Fig. 4). The wobbling of three aromatic rings at 303 K was considered to cause broadening of the signals by an equilibrium between different conformations and/or changing of anisotropic effects

Table 1 X-Ray calculated backbone dihedrals in compound **1**, RA-VI and RA-V-*p*-bromobenzoate

Residue	Dihedral angle/°	Compound **1**	RA-VI[a]	RA-V-*p*-bromobenzoate[b]
D-Ala-1	φ	128.7(6)	137.9(6)	137.8(17)
	ψ	−149.3(6)	−142.2(6)	−169.7(13)
	ω	176.4(5)	−177.4(5)	−175.3(15)
Ala-2, (Ser-2)[c]	φ	−86.3(7)	−115.8(7)	−83.1(19)
	ψ	142.9(6)	90.7(9)	120.9(16)
	ω	179.0(5)	−174.0(5)	−178.3(14)
D-Tyr-3, (Tyr-3)[d]	φ	120.1(6)	102.3(9)	53.8(23)
	ψ	−105.9(6)	−51.4(11)	38.5(23)
	ω	−176.4(5)	172.8(6)	−167.9(13)
Ala-4	φ	−135.2(5)	−75.5(10)	−158.5(12)
	ψ	62.9(8)	162.9(6)	170.5(14)
	ω	168.4(5)	170.8(6)	174.1(12)
D-Tyr-5, (Tyr-5)[e]	φ	133.1(5)	−116.9(8)	−136.9(14)
	ψ	−98.7(6)	111.3(9)	101.7(17)
	ω	−174.9(5)	−1.0(13)	1.8(25)
Tyr-6	φ	−86.5(7)	−86.0(10)	−91.6(17)
	ψ	81.7(7)	161.2(6)	163.2(13)
	ω	174.3(5)	171.6(5)	171.4(13)

[a] Data given in reference 2. [b] Data given in reference 4. [c] Ser-2 in parentheses is that of RA-VI. [d] Tyr-3 in parentheses is that of RA-V-*p*-bromobenzoate. [e] Tyr-5 in parentheses are those of RA-VI and RA-V-*p*-bromobenzoate.

Table 2 Distances/Å between C5–C6, O2–C31 and C41–C5N in compound **1**, RA-VI and RA-V-*p*-bromobenzoate

	Distance/Å		
	C5–C6	O2–C31	C41–C5N
Compound **1**	3.855(11)	3.786(12)	4.425(13)
RA-VI	3.018(15)	3.936(14)	3.338(18)
RA-VII-*p*-Bromobenzoate	2.936(31)	3.092(32)	3.142(31)

Table 3 Lengths/Å of hydrogen bonding in X-ray structure of compound **1**[a]

Hydrogen bridge atom			
From	To	Symmetry	Lengths/Å
HN1	O5	(1)	2.10(10)
HN2	O3	(2)	2.04(12)
HN4	O1W	(1)	1.89(10)
O1W	O2W	(3)	2.951(15)
O2W	O1	(1)	3.159(18)
O2W	O2	(2)	2.890(17)

[a] Equivalent position: (1) x, y, z, (2) $\frac{1}{2}+x, \frac{1}{2}-y, -z$, (3) $-\frac{1}{2}+x, \frac{1}{2}-y, -z$.

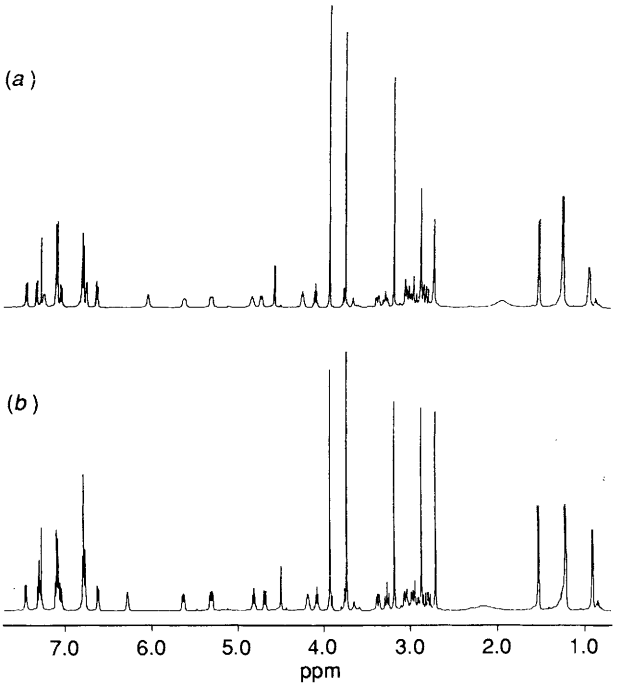

Fig. 4 500 MHz ^{1}H NMR spectra of compound **2** in $CDCl_3$; (*a*) measured at 303 K. Some broad signals are observed; (*b*) measured at 273 K. The broad signals seen in (*a*) are sharp now.

of the aromatic rings. The ^{1}H signals of the β-turn of Ala-2 and Tyr-3 in compounds **3** and **4** were quite similar to those in the minor conformer of RA-VII, which has a *cis* *N*-methyl amide bond between Ala-2 and Tyr-3. The *N*-methyl signals of Tyr-6 of compounds **1**–**4** all showed a slight low field shift when compared with the corresponding signals of RAs, having a *cis* *N*-methyl peptide bond between Tyr-5 and -6. This small difference is considered to be caused by the decreased anisotropic effect of Tyr-5 aromatic ring by the isomerization of L-Tyr-5 to D-Tyr-5 and the isomerization of the *N*-methyl amide bond from *cis* to *trans* (see below).

In the ^{13}C signals, compounds **1** and **2** did not show a lower field chemical shift for the Tyr-3-Cα signal, which RAs characteristically show,[8] and their chemical shift patterns were similar to those of RA-VI. Compounds **3** and **4** also showed signals similar to those of the minor conformer of RA-VII. The signal of Tyr-5-Cα tended to resonate at a lower field than the corresponding signals of RA-VI and VII.

On the basis of the chemical shifts of the ^{1}H and ^{13}C NMR signals described above, in compounds **1**–**4**, Tyr-5 was shown to have been isomerized to the D-form and the *N*-methyl amide bond between Tyr-5 and Tyr-6 to *trans*. Compounds **1** and **2** were then considered to be isomerized to the D-form at Tyr-3 and compounds **3** and **4** were isomerized to *cis* between Ala-2 and Tyr-3.

Table 4 ^{1}H-NMR chemical shifts of compounds **1**–**4** in $CDCl_3$ at 303 K (500 MHz)[a]

Amino acid	Proton	1	2	3	4
D-Ala-1	H_α	4.46, $J_{\alpha\beta}$ = 6.2	4.10, $J_{\alpha\beta}$ = 7.1	4.34, $J_{\alpha\beta}$ = 7.0	4.43, $J_{\alpha\beta}$ = 6.9
	H_β	1.27, $J_{\alpha N}$ = 8.1	1.26, $J_{\alpha N}$ = *	1.21, $J_{\alpha N}$ = 8.0	1.26, $J_{\alpha N}$ = 7.6
	H_N	7.12	7.22	6.85	6.56
Ala-2	H_α	4.64, $J_{\alpha\beta}$ = 7.0	4.25, $J_{\alpha\beta}$ = 5.2	4.25, $J_{\alpha\beta}$ = 6.7	4.39, $J_{\alpha\beta}$ = 6.6
	H_β	0.97, $J_{\alpha N}$ = 7.6	0.96, $J_{\alpha N}$ = *	0.49, $J_{\alpha N}$ = *	0.57, $J_{\alpha N}$ = 8.2
	H_N	7.18	6.03	6.44	7.42
D-Tyr-3 (Tyr-3)[b]	H_α	5.14, $J_{\alpha\beta1}$ = 8.5	5.60, $J_{\alpha\beta1}$ = 10.8	4.94, $J_{\alpha\beta1}$ = 11.5	4.88, $J_{\alpha\beta1}$ = 10.7
	$H_{\beta1(pro-R)}$	3.11, $J_{\alpha\beta2}$ = 8.5	2.82, $J_{\alpha\beta2}$ = 5.6	3.00, $J_{\alpha\beta2}$ = 3.2	3.05, $J_{\alpha\beta2}$ = 4.1
	$H_{\beta2(pro-S)}$	2.95, $J_{\beta1\beta2}$ = 14.3	3.37, $J_{\beta1\beta2}$ = 15.2	3.51, $J_{\beta1\beta2}$ = 14.8	2.95, $J_{\beta1\beta2}$ = 14.5
	$2H_\delta$	7.06, $J_{\delta\varepsilon}$ = 8.6	7.08, $J_{\delta\varepsilon}$ = 8.6	7.08, $J_{\delta\varepsilon}$ = 8.6	7.03, $J_{\delta\varepsilon}$ = 8.6
	$2H_\delta$	6.77	6.78	6.82	6.82
	Me_N	3.09	2.88	2.87	2.92
	Me_O	3.73	3.74	3.74	3.75
Ala-4	H_α	4.87, $J_{\alpha\beta}$ = 6.1	4.83, $J_{\alpha\beta}$ = 7.0	4.89, $J_{\alpha\beta}$ = 6.5	4.93, $J_{\alpha\beta}$ = 6.5
	H_β	1.25, $J_{\alpha N}$ = 8.6	1.53, $J_{\alpha N}$ = 5.9	1.41, $J_{\alpha N}$ = 6.7	1.42, $J_{\alpha N}$ = 8.2
	H_N	6.90	6.74	7.14	8.03
D-Tyr-5	H_α	5.59, $J_{\alpha\beta1}$ = 4.2	5.29, $J_{\alpha\beta1}$ = *	5.69, $J_{\alpha\beta1}$ = 5.1	5.28, $J_{\alpha\beta1}$ = 5.4
	$H_{\beta1(pro-S)}$	2.84, $J_{\alpha\beta2}$ = 11.6	3.00, $J_{\alpha\beta2}$ = 11.9	3.00, $J_{\alpha\beta2}$ = 11.9	3.13, $J_{\alpha\beta2}$ = 12.0
	$H_{\beta2(pro-R)}$	3.25, $J_{\beta1\beta2}$ = 11.6	3.29, $J_{\beta1\beta2}$ = 11.9	3.37, $J_{\beta1\beta2}$ = 11.9	3.32, $J_{\beta1\beta2}$ = 12.0
	$H_{\delta1}$	7.28, $J_{\delta1\delta2}$ = 2.1	7.31, $J_{\delta1\delta2}$ = 2.0	7.30, $J_{\delta1\delta2}$ = 2.1	7.27, $J_{\delta1\delta2}$ = 1.4
	$H_{\delta2}$	7.43, $J_{\delta1\varepsilon1}$ = 8.3	7.43, $J_{\delta1\varepsilon1}$ = 8.3	7.42, $J_{\delta1\varepsilon1}$ = 8.4	7.41, $J_{\delta1\varepsilon1}$ = 8.6
	$H_{\varepsilon1}$	6.96, $J_{\delta2\varepsilon2}$ = 8.5	7.03, $J_{\delta2\varepsilon2}$ = 8.5	7.01, $J_{\delta2\varepsilon2}$ = 8.5	7.06, $J_{\delta2\varepsilon2}$ = 9.0
	$H_{\varepsilon2}$	7.03, $J_{\varepsilon1\varepsilon2}$ = 2.4	7.08, $J_{\varepsilon1\varepsilon2}$ = 2.4	* $J_{\varepsilon1\varepsilon2}$ = 2.4	7.06, $J_{\varepsilon1\varepsilon2}$ = 2.1
	Me_N	2.92	3.18	3.26	3.21
Tyr-6	H_α	4.57, $J_{\alpha\beta1}$ = 11.6	4.73, $J_{\alpha\beta1}$ = *	4.65, $J_{\alpha\beta1}$ = 11.7	4.44, $J_{\alpha\beta1}$ = 12.6
	$H_{\beta1(pro-R)}$	3.15, $J_{\alpha\beta2}$ = 0.0	2.95, $J_{\alpha\beta2}$ = *	3.00, $J_{\alpha\beta2}$ = 2.3	2.82, $J_{\alpha\beta2}$ = 3.6
	$H_{\beta2(pro-S)}$	2.80, $J_{\beta1\beta2}$ = 19.0	2.95, $J_{\beta1\beta2}$ = *	3.00, $J_{\beta1\beta2}$ = *	3.29, $J_{\beta1\beta2}$ = 12.6
	$H_{\delta1}$	6.58, $J_{\delta1\delta2}$ = 1.8	6.62, $J_{\delta1\delta2}$ = 1.8	6.60, $J_{\delta1\delta2}$ = 1.9	6.61, $J_{\delta1\delta2}$ = 2.0
	$H_{\delta2}$	4.49, $J_{\delta1\varepsilon1}$ = 8.3	4.58, $J_{\delta1\varepsilon1}$ = 8.3	4.53, $J_{\delta1\varepsilon1}$ = 8.3	4.51, $J_{\delta1\varepsilon1}$ = 8.3
	$H_{\varepsilon1}$	6.77	6.79	6.96	6.79
	Me_N	2.75	2.73	2.88	2.96
	Me_O	3.91	3.93	3.92	3.92

[a] *J*-Values are given in Hz. [b] The residue 3 of compounds **3** and **4** is Tyr-3. Asterisks were not determined in the present study.

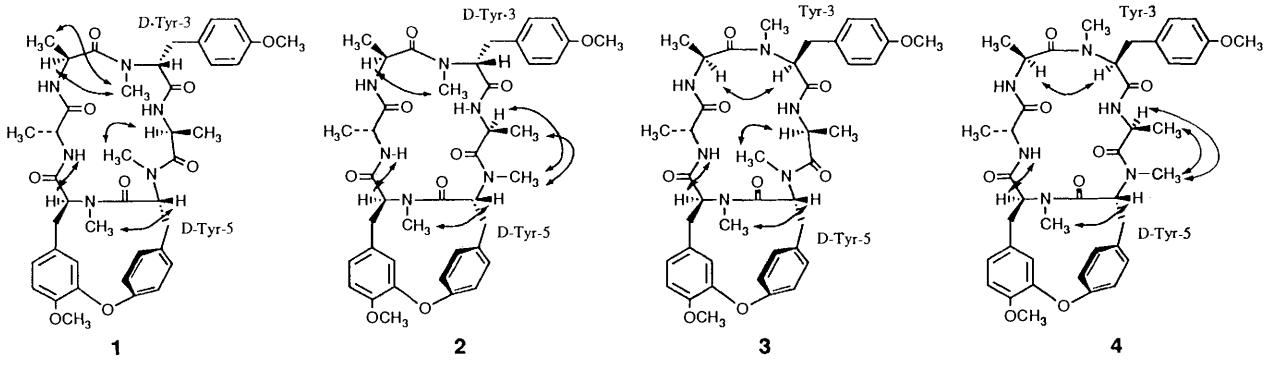

Fig. 5 NOE enhancements of compounds **1**–**4**. The arrows show the NOE relationships confirmed by NOESYPH experiments in $CDCl_3$ at 303 K.

Detailed conformational studies are necessary for an understanding of the biological action of this family. Therefore, a structural and conformational analysis of compounds **1**–**4** in solution was made by the following experiments.

NOE enhancements. The NOE enhancements observed in compounds **1**–**4** in NOESYPH[19] spectra are shown in Fig. 5. The NOE enhancements between D-Tyr-3-NCH_3 and Ala-2-Hα/Ala-2-CH_3 of compound **1** proved their relative structure in the solid state, *i.e.*, type V β-turn, revealed by X-ray analysis. The NOE enhancements between Tyr-6-NCH_3 and Tyr-5-Hα observed in compounds **1**–**4**, indicated that Tyr-5 is in the D-form and that the *N*-methyl amide bond between Tyr-5 and Tyr-6 was *trans*. Because of the inversion of ψ and φ angles in Ala-4 and Tyr-5, respectively, NOE was observed between Tyr-5-NCH_3 and Ala-4-Hα but not between Tyr-5-NCH_3 and Ala-4-CH_3. These correlations showed that the conformation of compound **1** in solution estimated from the NMR data is almost identical with that of the crystalline state. In the NOE relationship of compound **2**, the cross peak between Tyr-3-NCH_3 and Ala-2-Hα supports the formation of a type II β-turn similar to that of RA-VI. What distinguishes compound **2** from compound **1** is the presence of NOEs both between Tyr-5-NCH_3 and Ala-4-Hα, and between Tyr-5-NCH_3 and Ala-4-CH_3, indicating that the ψ and φ angles in Ala-4 and D-Tyr-5, respectively, are changing around the *N*-methyl amide bond. In the NOEs of compound **3** (except for the NOE between Ala-2-Hα and Tyr-3-Hα, suggesting that the *cis* *N*-methyl amide bond between Ala-2 and Tyr-3 is similar to a minor conformer

Table 5 ^{13}C NMR chemical shifts of compounds **1**–**4** in $CDCl_3$ at 303 K (125 MHz)

Amino acid	Carbon	1	2	3	4
D-Ala-1	C_α	47.93	49.19	48.43	47.78
	C_β	18.03	17.23	19.22	18.25
	$C_{C=O}$	171.39	173.00	172.38	172.82
Ala-2	C_α	43.03	46.03	44.31	43.51
	C_β	17.37	15.78	17.03	16.69
	$C_{C=O}$	174.37	173.00	174.26	172.17
D-Tyr-3	C_α	56.95	57.14	63.18	62.00
(Tyr-3)[a]	C_β	33.35	32.67	33.75	33.84
	C_γ	130.52	*	130.24	130.05
	C_δ	129.88	129.83	130.24	130.26
	C_ε	113.85	113.83	114.51	114.44
	C_ζ	158.53	158.34	158.82	158.76
	$C_{C=O}$	168.52	171.30	168.97	168.28
	C_N	30.50	30.88	30.12	29.07
	C_O	55.22	55.26	55.33	55.34
Ala-4	C_α	45.96	52.28	47.71	46.42
	C_β	17.61	17.42	17.61	17.82
	$C_{C=O}$	171.00	171.30	171.91	172.50
D-Tyr-5	C_α	57.36	58.50	55.33	55.91
	C_β	35.67	35.28	35.69	35.92
	C_γ	134.43	133.80	133.57	132.93
	$C_{\delta1}$	133.14	133.38	133.15	132.83
	$C_{\delta2}$	130.85	130.50	130.47	130.41
	$C_{\varepsilon1}$	123.95	124.10	124.12	124.02
	$C_{\varepsilon2}$	124.38	124.85	125.07	125.97
	C_ζ	156.61	156.99	157.07	157.43
	$C_{C=O}$	170.24	171.12	171.12	171.84
	C_N	29.99	32.26	30.46	31.52
Tyr-6	C_α	56.41	56.64	56.72	59.18
	C_β	29.89	29.94	30.22	33.24
	C_γ	128.17	129.13	129.26	129.01
	$C_{\delta1}$	121.45	121.57	121.59	121.25
	$C_{\delta2}$	113.02	113.46	113.27	113.60
	$C_{\varepsilon1}$	112.06	112.12	112.14	112.24
	$C_{\varepsilon2}$	152.60	152.56	152.48	152.40
	C_ζ	146.42	146.45	146.36	146.20
	$C_{C=O}$	170.71	170.18	170.42	171.31
	C_N	30.03	30.45	30.78	31.23
	C_O	56.16	56.23	56.19	56.21

[a] The residue 3 of compounds **3** and **4** is Tyr-3. Asterisks were not determined in the present study.

Table 6 Effect of temperature on the NH chemical shifts of compounds **1**–**4** in $[^2H_6]$DMSO, $-\Delta\delta/\Delta T$ (10^3 ppm/K)

Compounds	D-Ala-1	Ala-2	Ala-4
1	4.5	4.5	8.5
2	2.8	5.8	1.3
3	1.5	3.8	6.5
4	−0.3	4.6	3.6

in RA-VII), the same relationship to compound **1** was observed. Compound **4** was also shown by NOE to possess a *cis* *N*-methyl amide bond between Ala-2 and Tyr-3. Furthermore, the presence of NOEs both between Tyr-5-NCH_3 and Ala-4-Hα, and between Tyr-5-NCH_3 and Ala-4-CH_3 revealed the same relationship to compound **2**. However, broad signals as in compound **2** were not observed. The amount of minor conformer in RA-VII was increased in DMSO solution.[9] The fact that in DMSO the yield of compounds **3** and **4** with *cis* *N*-methyl amide bonds was increased and that Tyr-3 was not isomerized could be explained by the steric stability around the *cis* *N*-methyl amide bond between Ala-2 and Tyr-3.

Temperature dependence of NH chemical shifts. For the determination of the secondary structure of peptides in solution by NMR spectroscopy, it must be determined which NH protons are exposed to the solvent and which ones are shielded from the solvent, either sterically or through hydrogen bonding. The most common procedure for that purpose is to determine the temperature effects on the NH protons[20] in $[^2H_6]$DMSO solution, an hydrogen accepting solvent.

The temperature coefficients ($\Delta\delta/\Delta T$) of compounds **1**–**4** are given in Table 6. It is clearly shown that D-Ala-1-NH in compounds **1** and **3** are shielded from the solvent, whereas Ala-2-NH and Ala-4-NH are exposed to the solvent. Compounds **1** and **3** are considered to possess the γ-turn conformations with hydrogen bonding between D-Ala-1-NH and D-Tyr-5-CO,[21] and not an antiparallel β-pleated conformation stabilized by 4-1 type hydrogen bonds. On the other hand, Ala-4-NH in compound **2** is strongly shielded from the solvent, suggesting that it has a type II β-turn stabilized by the hydrogen bond between Ala-4-NH and D-Ala-1-CO. In compound **4**, a strong hydrogen bond between D-Ala-1-NH and Ala-4-CO and a weak one between Ala-4-NH and D-Ala-1-CO were suggested by the temperature coefficients.

Antitumour Activity.—RAs and the related compounds, bouvardins, have been shown to inhibit protein synthesis through eukaryotic 80S ribosomal binding, resulting in inhibition of aminoacyl-tRNA binding and peptidyl-tRNA translocation, which is presently regarded as the site of action for these antitumour agents.[10]

As regards the role of the 14-membered *N*-methylcycloisodityrosine subunit, early studies[22] suggested that the 14-membered *N*-methylcycloisodityrosine subunit might potentiate the cytotoxic and antitumour properties of the D-Ala-Ala-*N*(Me)-Tyr(OMe)-Ala segment of RAs by serving as the scaffolding for maintaining its active, normally inaccessible conformation within the 18-membered ring. We have shown that O-*seco*-RA-VII (RA-VII-H)[8] lacks the biological properties of RA-VII, as O-*seco*-deoxybouvardin,[23] as stated by Bates and Boger *et al.* Furthermore, modification of functional groups of the 14-membered cyclic dipeptide segment of RAs changes its antitumour activities,[3,4] especially when an α-proton at the Cβ position of Tyr-6 is replaced by a bulky substituent group,[4] when a remarkable decrease of antitumour activity is observed. This result leads to the suggestion that the introduction of large substituent groups at the α-side of RAs inhibits its eukaryotic 80S ribosomal binding.

In our preliminary paper,[8] we stated that the 14-membered ring was necessary for the antitumour activity and that the conformation of 18-membered ring produced by the *cis*/*trans* isomerization of the *N*-methyl amide bond at residues 2 and 3 intensively enhanced their biological properties. In RAs, the proportion of the conformation with *cis* geometry between Ala-2 and Tyr-3 was increased in polar solvents such as $[^2H_6]$DMSO.[8,9] In addition, the steric increment of the side chain at residue 2, in RA-III, VIII, IX and X, decreased the cytotoxic and antitumour activities.[1,4,5]

In compounds **1**–**4**, obtained in this work, only compounds **3** and **4**, having a *cis* *N*-methyl amide bond between Ala-2 and Tyr-3, showed *in vivo* antitumour activities without causing body weight loss at higher dose than that of RA-VII (Table 7). Compounds **3**, **4** and the minor conformer of RA-VII have a similar local conformation at their β-turn region, constructed by Ala-2 and Tyr-3, but a different orientation in the *N*-methyl amide bond between Tyr-5 and Tyr-6 (RA-VII: *cis*; compounds **3** and **4**: *trans*). This difference is evidently shown by the NOE enhancements of the three compounds. The *cis* *N*-methyl amide bond between residues 5 and 6 was said to be necessary for the compound to show antitumour activity.[24] However,

compounds **3** and **4**, whose *N*-methyl amide bond between residues 5 and 6 was *trans*, exhibited antitumour properties, which suggests that the *cis* geometry between residues 5 and 6 is *not* an essential requirement for the activity. We reported that RA-IX[1] and [*N*-demethyl-Tyr-3(OCH_3)]RA-VII,[25] whose *N*-methyl amide bonds between residues 2 and 3 are restricted to *trans*, abolished *in vivo* antitumour activities. We consider that the *cis* geometry between residues 2 and 3 (type VI β-turn) is necessarily the preference to the *trans N*-methyl amide bond (type II β-turn) to show activity. Here, we suggest the *cis N*-methyl amide bond between residues 2 and 3 plays an important role in antitumour activity. It is, however, easy to transform between the *cis* and *trans N*-methyl amide bonds, because the isomerization energy barrier is very low (*ca.* 18.0 kcal mol^{-1})[26] and the binding receptor on ribosome 80S might not be rigid. Studies on the synthesis of conformationally constrained derivatives and their activities are in progress.

Experimental

General details.—M.p.s were determined on a Yanagimoto micro-melting point apparatus and are uncorrected. Optical rotations were measured with a JASCO DIP-4 spectrometer, $[\alpha]_D$ values are given in 10^{-1} deg cm^2 g^{-1}. Mass spectra were taken with a Hitachi M-80 spectrometer. UV and IR spectra were recorded on a Hitachi 557 spectrophotometer and a Perkin-Elmer 1710 spectrophotometer, respectively. Medium-

Table 7 Antitumour activities of compounds **1**–**4** on P388 leukaemia[a]

Compounds	Dose (mg kg^{-1})	*T*/C (%)
1	25.0	[b]
2	25.0	[b]
3	25.0	122
	35.0	135
4	3.0	153
	15.0	168

[a] P388 was introduced into the peritoneal cavity of (1×10^6 cells cm^{-3}) CDF1 mice on day 0. Drugs suspended in 0.5% CMC–saline were given daily at indicated doses intra peritoneally for 9 consecutive days starting on day 1. [b] Not active.

Table 9 Bond lengths/Å with estimated standard deviations in parentheses for compound **1**

Bond	Distance/Å	Bond	Distance/Å
N(1)–C(1)	1.47(1)	C(40)–N(5)	1.36(1)
N(1)–C(60)	1.33(1)	N(5)–C(5N)	1.47(1)
C(1)–C(10)	1.56(1)	N(5)–C(5)	1.49(1)
C(1)–C(11)	1.51(1)	C(5)–C(50)	1.56(1)
C(10)–O(1)	1.22(1)	C(5)–C(51)	1.57(1)
C(10)–N(2)	1.34(1)	C(50)–O(5)	1.20(1)
N(2)–C(2)	1.48(1)	C(50)–N(6)	1.36(1)
C(2)–C(20)	1.53(1)	C(51)–C(52)	1.51(1)
C(2)–C(21)	1.54(1)	C(52)–C(53)	1.40(1)
C(20)–O(2)	1.20(1)	C(52)–C(57)	1.43(1)
C(20)–N(3)	1.33(1)	C(53)–C(54)	1.41(1)
N(3)–C(3N)	1.47(1)	C(54)–C(55)	1.32(2)
N(3)–C(3)	1.49(1)	C(55)–C(56)	1.44(1)
C(3)–C(30)	1.55(1)	C(55)–O(51)	1.40(1)
C(3)–C(31)	1.56(1)	C(56)–C(57)	1.38(1)
C(30)–O(3)	1.23(1)	O(51)–C(64)	1.41(1)
C(30)–N(4)	1.35(1)	N(6)–C(6N)	1.48(1)
C(31)–C(32)	1.50(1)	N(6)–C(6)	1.49(1)
C(32)–C(33)	1.39(2)	C(6)–C(60)	1.56(1)
C(32)–C(37)	1.39(1)	C(6)–C(61)	1.57(1)
C(33)–C(34)	1.43(2)	C(60)–O(6)	1.21(1)
C(34)–C(35)	1.39(2)	C(61)–C(62)	1.52(1)
C(35)–C(36)	1.40(2)	C(62)–C(63)	1.36(1)
C(35)–O(31)	1.38(1)	C(62)–C(67)	1.38(1)
C(36)–C(37)	1.36(2)	C(63)–C(64)	1.37(1)
O(31)–C(38)	1.42(1)	C(64)–C(65)	1.40(1)
N(4)–C(4)	1.46(1)	C(65)–C(66)	1.36(1)
C(4)–C(40)	1.54(1)	C(65)–O(61)	1.38(1)
C(4)–C(41)	1.53(1)	C(66)–C(67)	1.42(1)
C(40)–O(4)	1.23(1)	O(61)–C(68)	1.42(1)

Table 8 Fractional atomic co-ordinates ($\times 10^4$) with estimated standard deviations in parentheses for compound **1**

Atom	*x*	*y*	*z*	Atom	*x*	*y*	*z*
N(1)	4217(6)	1099(2)	924(8)	N(5)	6356(5)	2030(2)	3377(6)
C(1)	3785(7)	1256(3)	−319(9)	C(5N)	6583(8)	2047(3)	1958(8)
C(10)	4412(7)	1634(3)	−859(9)	C(5)	6400(6)	1589(2)	4023(8)
O(1)	5262(5)	1624(3)	−713(9)	C(50)	5740(6)	1260(2)	3287(8)
C(11)	3732(8)	900(3)	−1364(11)	O(5)	6030(4)	1070(2)	2327(6)
N(2)	3943(5)	1941(2)	−1544(7)	C(51)	7432(6)	1408(3)	4069(10)
C(2)	4465(6)	2330(3)	−2034(9)	C(52)	7389(6)	992(2)	4872(10)
C(20)	4456(7)	2660(3)	−888(9)	C(53)	7450(7)	590(3)	4211(10)
O(2)	3747(5)	2707(3)	−244(8)	C(54)	7141(7)	207(3)	4855(11)
C(21)	3985(7)	2522(3)	−3271(9)	C(55)	6765(7)	227(3)	6048(11)
N(3)	5231(5)	2901(2)	−711(7)	C(56)	6792(8)	621(3)	6839(10)
C(3N)	6090(8)	2867(3)	−1522(11)	C(57)	7108(7)	1000(3)	6232(10)
C(3)	5218(7)	3228(2)	389(8)	O(51)	6223(5)	−121(2)	6546(8)
C(30)	6019(6)	3115(2)	1381(8)	N(6)	4878(5)	1189(2)	3836(7)
O(3)	6857(4)	3180(2)	1131(6)	C(6N)	4454(8)	1443(3)	4932(12)
C(31)	5323(8)	3709(3)	−130(9)	C(6)	4283(6)	846(2)	3195(9)
C(32)	5291(7)	4029(2)	993(9)	C(60)	3718(6)	1060(2)	2038(10)
C(33)	4450(8)	4148(3)	1597(11)	O(6)	2903(5)	1167(2)	2180(8)
C(34)	4431(8)	4456(3)	2668(12)	C(61)	3575(7)	604(3)	4139(10)
C(35)	5280(8)	4642(3)	3076(10)	C(62)	3980(6)	289(2)	5160(9)
C(36)	6121(7)	4511(3)	2477(11)	C(63)	4922(7)	247(3)	5404(10)
C(37)	6127(7)	4206(3)	1486(11)	C(64)	5258(7)	−55(3)	6298(9)
O(31)	5351(5)	4961(2)	4049(7)	C(65)	4634(7)	−332(3)	6973(9)
C(38)	4504(9)	5090(3)	4693(11)	C(66)	3693(7)	−294(3)	6718(9)
N(4)	5714(5)	2934(2)	2529(6)	C(67)	3346(7)	15(3)	5790(10)
C(4)	6397(6)	2838(2)	3567(8)	O(61)	5050(5)	−629(2)	7829(7)
C(40)	6251(6)	2383(2)	4187(8)	C(68)	4421(9)	−874(3)	8643(11)
O(4)	6052(5)	2347(2)	5371(6)	O(1W)	3660(7)	2698(6)	3035(9)
C(41)	6348(8)	3191(3)	4643(10)	O(2W)	7426(11)	1778(5)	−1286(13)

Table 10 Bond angles/° with estimated deviations in parentheses for compound **1**

Bond	Angle/°	Bond	Angle/°
C(1)–N(1)–C(60)	121.6(7)	C(40)–N(5)–C(5)	117.1(6)
C(10)–C(1)–N(1)	107.5(7)	C(50)–C(5)–N(5)	110.3(6)
C(10)–C(1)–C(11)	108.5(8)	C(50)–C(5)–C(51)	110.4(6)
N(1)–C(1)–C(11)	112.3(8)	N(5)–C(5)–C(51)	111.7(6)
O(1)–C(10)–C(1)	120.4(9)	O(5)–C(50)–C(5)	119.1(7)
O(1)–C(10)–N(2)	125.0(9)	O(5)–C(50)–N(6)	124.0(7)
C(1)–C(10)–N(2)	114.4(8)	C(5)–C(50)–N(6)	116.7(7)
C(2)–N(2)–C(10)	118.7(7)	C(52)–C(51)–C(5)	106.0(7)
C(20)–C(2)–N(2)	105.7(7)	C(53)–C(52)–C(51)	118.7(8)
C(20)–C(2)–C(21)	110.9(7)	C(53)–C(52)–C(57)	119.4(8)
N(2)–C(2)–C(21)	110.7(7)	C(51)–C(52)–C(57)	120.8(8)
O(2)–C(20)–C(2)	119.4(8)	C(54)–C(53)–C(52)	119.3(9)
O(2)–C(20)–N(3)	123.4(9)	C(55)–C(54)–C(53)	120.5(9)
C(2)–C(20)–N(3)	117.0(8)	C(56)–C(55)–C(54)	122.3(9)
C(3N)–N(3)–C(20)	124.8(8)	C(56)–C(55)–O(51)	116.6(8)
C(3N)–N(3)–C(3)	118.1(7)	C(54)–C(55)–O(51)	120.8(9)
C(20)–N(3)–C(3)	117.2(7)	C(57)–C(56)–C(55)	117.4(9)
C(30)–C(3)–N(3)	108.7(7)	C(64)–O(51)–C(55)	111.2(7)
C(30)–C(3)–C(31)	110.7(7)	C(6N)–N(6)–C(50)	126.0(7)
N(3)–C(3)–C(31)	112.2(7)	C(6N)–N(6)–C(6)	117.4(7)
O(3)–C(30)–C(3)	122.6(7)	C(50)–N(6)–C(6)	116.4(6)
O(3)–C(30)–N(4)	123.4(7)	C(60)–C(6)–N(6)	108.7(6)
C(3)–C(30)–N(4)	114.0(7)	C(60)–C(6)–C(61)	108.8(7)
C(32)–C(31)–C(3)	110.9(7)	N(6)–C(6)–C(61)	115.5(7)
C(33)–C(32)–C(31)	122.0(8)	O(6)–C(60)–N(1)	125.7(8)
C(33)–C(32)–C(37)	118.3(9)	O(6)–C(60)–C(6)	121.0(8)
C(31)–C(32)–C(37)	119.7(8)	N(1)–C(60)–C(6)	113.3(7)
C(34)–C(33)–C(32)	121.3(9)	C(62)–C(61)–C(6)	117.7(7)
C(35)–C(34)–C(33)	118.2(9)	C(63)–C(62)–C(61)	123.5(8)
C(36)–C(35)–C(34)	119.7(9)	C(63)–C(62)–C(67)	119.9(8)
C(36)–C(35)–O(31)	116.5(8)	C(61)–C(62)–C(67)	116.5(8)
C(34)–C(35)–O(31)	123.9(9)	C(64)–C(63)–C(62)	121.4(9)
C(37)–C(36)–C(35)	121.2(9)	C(65)–C(64)–O(51)	116.3(8)
C(38)–O(31)–C(35)	117.2(8)	C(65)–C(64)–C(63)	120.2(8)
C(4)–N(4)–C(30)	118.9(6)	O(51)–C(64)–C(63)	123.4(8)
C(40)–C(4)–N(4)	112.6(6)	C(66)–C(65)–C(64)	118.5(8)
C(40)–C(4)–C(41)	110.0(7)	C(66)–C(65)–O(61)	126.1(8)
N(4)–C(4)–C(41)	109.7(7)	C(64)–C(65)–O(61)	115.4(8)
O(4)–C(40)–C(4)	120.2(7)	C(67)–C(66)–C(65)	121.4(9)
O(4)–C(40)–N(5)	122.6(7)	C(68)–O(61)–C(65)	115.8(8)
C(4)–C(40)–N(5)	117.2(7)	C(32)–C(37)–C(36)	121.2(9)
C(5N)–N(5)–C(40)	125.6(7)	C(52)–C(57)–C(56)	120.0(9)
C(5N)–N(5)–C(5)	116.5(6)	C(62)–C(67)–C(66)	118.6(8)

pressure liquid chromatography (MPLC) was performed with a CIG column system (22 mm i.d. × 100 mm, Kusano Scientific Co., Tokyo) packed with 10 μm silica gel. High-pressure liquid chromatography (HPLC) was performed with a Inertsil PREP-ODS column (20 mm i.d. × 250 mm, Gasukuro Kogyo Inc.) packed with 10 μm ODS. TLC was conducted on precoated Kieselgel 60 F_{254} (Art. 5715; Merck). Spots on TLC were detected by their absorption under UV light. NMR coupling constants, *J*-values are given in Hz.

Materials. RA-VII used in this experiment was isolated from *Rubia cordifolia* by the procedure cited in reference 2.

NMR spectra. ^1H and ^{13}C NMR spectra were recorded on Bruker spectrometers (AM400 and AM500) and processed on a Bruker data station with an Aspect 3000 computer. Samples (10 mg) of compounds **1**–**4** in $CDCl_3$ or [$^2H_6$]DMSO (0.5 cm^3) in a 5 mm tube was used for the homonuclear measurement and samples (30 mg) in $CDCl_3$ or [$^2H_6$]DMSO (0.5 cm^3) in a 5 mm tube for the heteronuclear measurement. The spectra were recorded at 303 K. NOESYPH experiments were made with a mixing time of 0.6 s.

Isomerization of RA-VII *to Compounds* **1**–**4**.—RA-VII (300 mg) was treated with 30% KOMe in methanol for a day. The reaction mixture was neutralized with dil. HCl and concentrated. The concentrate was subjected to MPLC with CH_2Cl_2–MeOH (30:1) and finally to HPLC with 70% MeOH to give compounds **1** (243 mg), **2** (8 mg) and **3** (24 mg), each as amorphous powders. When the reaction was carried out in DMSO, the yields of compounds **1**, **3** and **4** were 55, 7 and 20%, respectively, after the same purification procedure as mentioned above.

Compound **1**. M.p. 174–175 °C (from MeOH), $[\alpha]_D$ +83.1 (*c* 1.14, $CHCl_3$); *m/z* 770 (Found: 770.3668. Calc. for $C_{41}H_{50}N_6O_9$, M^+, 770.3638); ν_{max}(KBr)/cm^{-1} 3480 (NH) and 1641 (amide); λ_{max}(EtOH)/nm 276 (ε 3785).

Compound **2**. M.p. 183–185 °C (from MeOH), $[\alpha]_D$ +3.3 (*c* 0.24, $CHCl_3$); *m/z* 770 (Found: 770.3676. Calc. for $C_{41}H_{50}N_6O_9$, M^+, 770.3638); ν_{max}(KBr)/cm^{-1} 3476 (NH) and 1646 (amide); λ_{max}(EtOH)/nm 276 (ε 3210).

Compound **3**. M.p. 178–180 °C (from MeOH), $[\alpha]_D$ −14.3 (*c* 0.28, $CHCl_3$); *m/z* 770 (Found: 770.3688. Calc. for $C_{41}H_{50}N_6O_9$, M^+, 770.3638); ν_{max}(KBr)/cm^{-1} 3475 (NH) and 1645 (amide); λ_{max}(EtOH)/nm 277 (ε 3400).

Compound **4**. M.p. 188–190 °C (from MeOH), $[\alpha]_D$ +74.7 (*c* 0.34, $CHCl_3$); *m/z* 770 (Found: 770.3689. Calc. for $C_{41}H_{50}N_6O_9$, M^+, 770.3638); ν_{max}(KBr)/cm^{-1} 3480 (NH) and 1645 (amide); λ_{max}(EtOH)/nm 276 (ε 2640). The ^1H and ^{13}C NMR data of compounds **1**–**4** in $CDCl_3$ are shown in Tables 4 and 5.

Acid Hydrolysis of Compounds **1**–**4**.—Solutions of compounds **1**–**4** (each containing 5 mg of peptide) in 6 mol dm^{-3} HCl were heated at 110 °C for 14 h. After being cooled, each solution was concentrated to dryness. The residue was treated with 2% $NaHCO_3$ (1 cm^3) and 5 mmol dm^{-3} dansyl chloride in acetone (0.5 cm^3) at 37 °C for 1 h. At the same time, authentic amino acids of L-Ala and D-Ala were also treated with dansyl chloride in the same manner. The dansyl amino acids were subjected to HPLC under the following conditions: 4 mm i.d. × 250 mm (Nucleosil 5 μm) flow rate, 0.8 cm^3 min^{-1}, detection, λ/nm 340, solvent, 20% CH_3CN, 85 mmol dm^{-3} L-His, 5 mmol dm^{-3} $CH_3CO_2NH_4$, 25 mmol dm^{-3} $CuSO_4 \cdot 5H_2O$, pH 7.0. The t_R values were L-Ala, 12.3 and D-Ala, 13.1 min.

Crystallographic Analysis of Compound **1**.—Crystal data: $C_{41}H_{50}O_9N_6 \cdot 2H_2O$, orthorhombic, space group $P2_12_12_1$, Z = 4, a = 14.186(10), b = 30.483(21), c = 10.070(7) Å, V = 4355 $Å^3$, D_x = 1.231 g cm^{-3}, $F(000)$ = 1720. A crystal of *ca.* 0.7 × 0.5 × 0.8 mm in a thin walled glass capillary was mounted on a Philips four-circle diffractometer with graphite-monochromated CuKα radiation (μ 7.1 cm^{-1}) at 23 °C. A total of 3862 reflections were observed above the $2\sigma(I)$ level, with the 2θ range from 6–156°. The structure was determined by the direct method using the MULTAN program,[27] and the refinement was carried out by the block-diagonal-matrix least-squared method. The final R value was 0.089 [$R_w = \Sigma_w(|F_o| - |F_c|)^2/\Sigma w|F_o|^2 = 0.012$, where, $\sqrt{w} = 0.1$ when $|F_o| \leqq 2.5$, $\sqrt{w} = 1$ when $2.5 < |F_o| \leqq 60$, $\sqrt{w} = 60/|F_o|$ when $|F_o| > 60$] for the 3854 reflections. The number of atoms refined was 58 C, N and O atoms with anisotropic thermal parameters and 50 H atoms with isotropic parameters which were found on a difference electron-density map and located at calculated positions. No H atoms were assigned for solvate water molecules. Absolute configurations were deduced from those at C1 (D-Ala), C2 (L-Ala) and C4 (L-Ala) measured by the method of optical resolution. Final shift/esd values were ranged in 0.01–0.3 with the maximum value of 1.08 for O1W *y*-coordinate. The maximum residual electron densities were 0.89 and 0.52 e $Å^{-3}$ found close to O1W: remaining residual peaks were less than 0.25 e $Å^{-3}$. The refined fractional atomic coordinates are shown in Table 8, the bond lengths in Table 9 and the bond angles in Table 10. The molecular structure determined by this method is illustrated in Fig. 2. Hydrogen-

atom coordinates and thermal parameters have been deposited at the Cambridge Crystallographic Data Centre (CCDC).*

* For details of the CCDC deposition scheme, see 'Instructions for Authors,' *J. Chem. Soc., Perkin Trans. 2*, 1992, issue 1.

References

1 Part 3, H. Itokawa, T. Yamamiya, H. Morita and K. Takeya, *J. Chem. Soc., Perkin Trans. 1*, 1992, 455.
2 H. Itokawa, K. Takeya, K. Mihara, N. Mori, T. Hamanaka, T. Sonobe and Y. Iitaka, *Chem. Pharm. Bull.*, 1983, **31**, 1424; H. Itokawa, K. Takeya, N. Mori, T. Hamanaka, T. Sonobe and K. Mihara, *Chem. Pharm. Bull.*, 1984, **32**, 284.
3 H. Itokawa, K. Takeya, N. Mori, T. Sonobe, N. Serisawa, T. Hamanaka and S. Mihashi, *Chem. Pharm. Bull.*, 1984, **32**, 3216.
4 H. Itokawa, K. Takeya, N. Mori, T. Sonobe, S. Mihashi and T. Hamanaka, *Chem. Pharm. Bull.*, 1986, **34**, 3762.
5 H. Itokawa, H. Morita, K. Takeya, N. Tomioka, A. Itai and Y. Iitaka, *Tetrahedron*, 1991, **47**, 7007.
6 H. Morita, T. Yamamiya, K. Takeya and H. Itokawa, *Chem. Pharm. Bull.*, 1992, **40**, 1352.
7 H. Itokawa, H. Morita, K. Takeya, N. Tomioka and A. Itai, *Chem. Lett.*, 1991, 2217.
8 H. Morita, K. Kondo, Y. Hitotsuyanagi, K. Takeya, H. Itokawa, N. Tomioka, A. Itai and Y. Iitaka, *Tetrahedron*, 1991, **47**, 2757.
9 H. Itokawa, H. Morita and K. Takeya, *Chem. Pharm. Bull.*, 1992, **40**, 1050.
10 M. Zalacain, E. Zaera, D. Vazquez and A. Jimines, *FEBS Lett.*, 1982, **148**, 95.
11 S. Lam, F. Chow and A. Karmer, *J. Chromatogr.*, 1980, **199**, 295.
12 G. N. Ramachandran, C. Ramakrishnan and V. Sasisekharan, *J. Mol. Biol.*, 1963, **7**, 95.
13 D. S. Kemp and P. McNamara, *Tetrahedron Lett.*, 1982, **23**, 3701; D. S. Kempt and E. T. Sum, *Tetrahedron Lett.*, 1982, **23**, 3759.
14 G. Nemethy and M. P. Printz, *Macromolecules*, 1972, **6**, 755.
15 V. Madison, M. Atreyi, C. M. Deber and E. R. Blout, *J. Am. Chem. Soc.*, 1974, **96**, 6725; L. G. Pease and C. J. Watson, *J. Am. Chem. Soc.*, 1978, **100**, 1279; A. F. Spatola, M. K. Anwer, A. L. Rockwell and L. M. Gierasch, *J. Am. Chem. Soc.*, 1986, **108**, 825.
16 I. L. Karle, *J. Am. Chem. Soc.*, 1978, **100**, 1286.
17 A. Bax and S. Subramanian, *J. Magn. Reson.*, 1986, **67**, 565.
18 A. Bax and M. F. Summers, *J. Am. Chem. Soc.*, 1986, **108**, 2094.
19 G. Bodenhauser, H. Koger and R. R. Ernst, *J. Magn. Reson.*, 1984, **58**, 370.
20 See, for example: (*a*) H. Kessler, *Angew. Chem., Int. Ed. Engl.*, 1982, **94**, 509; *Angew. Chem. Int. Ed. Engl.*, 1982, **21**, 512; (*b*) A. Ravi, B. V. V. Prasad and P. Balaram, *J. Am. Chem. Soc.*, 1983, **105**, 105; (*c*) M. Iqbal and P. Balaram, *J. Am. Chem. Soc.*, 1981, **103**, 5548; (*d*) K. D. Kopple, M. Ohnishi and A. Go, *J. Am. Chem. Soc.*, 1969, **91**, 4264; (*e*) M. Ohnishi and D. W. Urry, *Biochem. Biophys. Res. Commun.*, 1969, **36**, 194.
21 Some examples: (*a*) M. A. Khaled, D. W. Urry and K. Okamoto, *Biochem. Biophys. Res. Commun.*, 1976, **72**, 162; (*b*) R. Kishore and P. Balaram, *Biopolymers*, 1985, **24**, 2041; (*c*) A. F. Spatola, M. K. Anwer, A. L. Rockwell and L. M. Gierasch, *J. Am. Chem. Soc.*, 1986, **108**, 825.
22 S. D. Jolad, J. J. Hoffmann, S. J. Torrance, R. M. Wiedhopf, J. R. Cale, S. K. Arore, R. B. Bates, R. L. Gargiulo and G. R. Kriek, *J. Am. Chem. Soc.*, 1977, **99**, 8040; R. B. Bates, J. R. Cole, J. J. Hoffmann, G. R. Kriek, G. S. Linz and S. J. Torrance, *J. Am. Chem. Soc.*, 1983, **105**, 1343.
23 R. B. Bates, G. L. Gin, M. A. Hassen, V. J. Hruby, K. D. Janda, G. R. Kriek, J.-P. Michaud and D. B. Vine, *Heterocycles*, 1984, **22**, 785; D. L. Boger and D. Yohannes, *J. Org. Chem.*, 1988, **53**, 487.
24 D. L. Boger and J. B. Myers, *J. Org. Chem.*, 1991, **56**, 5385.
25 H. Itokawa, K. Saitou, H. Morita and K. Takeya, *Chem. Pharm. Bull.*, 1991, **39**, 2161.
26 W. E. Stewart and T. H. Siddall, *Chem. Rev.*, 1970, **70**, 517; H. Kessler, *Angew. Chem.*, 1970, **82**, 237; (H. Kessler, *Angew. Chem., Int. Ed. Engl.*, 1970, **9**, 219); S. Sternhell, *Dynamic Nuclear Magnetic Resonance*, eds. L. M. Jackman and F. A. Cotton, Academic Press, New York, 1975, 163.
27 G. Germain, P. Main and M. M. Woolfson, *Acta Crystallogr., Sect. A*, 1971, **27**, 368.

Paper 2/00732K
Received 12*th February* 1992
Accepted 15*th May* 1992